Acta Mech 206, 53–57 (2009)
DOI 10.1007/s00707-008-0097-4

Vagesh D. Narasimhamurthy · Helge I. Andersson · Bjørnar Pettersen

Steady viscous flow past a tapered cylinder

Received: 4 October 2007 / Published online: 23 September 2008

Abstract The three-dimensional nature of the viscous flow past a linearly tapered circular cylinder is examined at low Reynolds numbers. The numerical solution of the unsteady Navier–Stokes equations converges to a steady state. The primary flow in planes perpendicular to the cylinder axis is practically indistinguishable from the two-dimensional flow past a uniform cylinder. A secondary spanwise flow is observed in the stagnation zone going from the wide end towards the narrow end, whereas a secondary motion on the rear side goes in the opposite direction. In spite of this secondary flow, the length of the separation zone varies linearly with the local Reynolds number.

1 Introduction

The flow past a circular cylinder with a uniform cross-section remains two-dimensional as long as the Reynolds number *Re* is below the critical value ≈ 190 beyond which the intrinsic 'mode A' instability is known to occur. If the diameter varies along the cylinder span, however, the diameter variation introduces inherent three-dimensionality into the flow. At Reynolds numbers of O(100), the wake flow becomes time-dependent and the local shedding frequency turns out to vary abruptly along the span either if the diameter changes discontinuously [1–3] or linearly [4–8]. For Reynolds numbers below $\approx$42, however, the wake behind a uniform cylinder is steady and the length of the closed wake is known to vary linearly with the Reynolds number.

The aim of this study is to examine the three-dimensional wake behind a linearly tapered circular cylinder at low Reynolds number. Both experiments [5] and simulations [6,8] have shown that even very modest tapering (taper ratio 75:1) gives rise to complex non-linear wake phenomena such as vortex splitting and dislocations for Reynolds numbers slightly above 100. Nevertheless, one may speculate whether the wake flow behind a slightly tapered cylinder can be considered as quasi-two-dimensional provided that the Reynolds number is lower than the critical value at which vortex shedding occurs. One may furthermore wonder how the secondary flow field, i.e. the departure from purely 2D behaviour, will appear. These issues will be addressed for the first time in the present study where we intentionally consider the same taper ratio for which complex three-dimensional wake phenomena have been observed at Reynolds numbers below the critical Reynolds number ≈ 190 at which intrinsic secondary instabilities are known to occur in the wake of uniform cylinders.

V. D. Narasimhamurthy (✉) · H. I. Andersson
Fluids Engineering Division, Department of Energy and Process Engineering,
Norwegian University of Science and Technology (NTNU), 7491 Trondheim, Norway,
E-mail: vagesh@ntnu.no
Tel.: +47-73593563
Fax.: +47-73593491

B. Pettersen
Department of Marine Technology, Norwegian University of Science and Technology, 7491 Trondheim, Norway

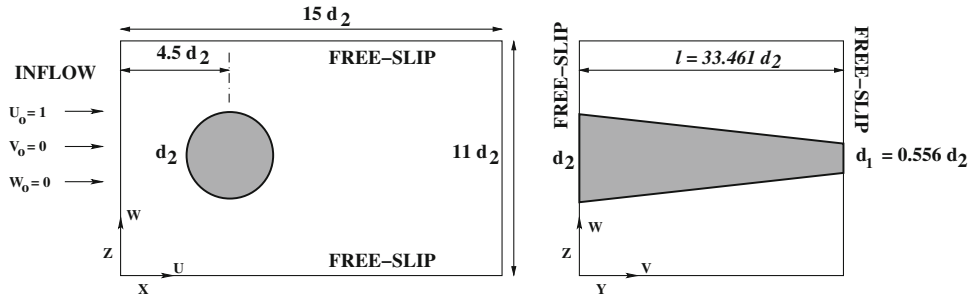

(a) Front view **(b)** Side view

Fig. 1 Computational domain (not to scale)

2 Problem formulation and numerical method

To this end we considered a circular cylinder with taper ratio $R_T = l/(d_2 - d_1) = 75$: 1 (where $l = 33.461 d_2$ is the length of the cylinder, and d_2 and $d_1 = 0.556 d_2$ denote the diameter of its wide and narrow ends, respectively). The size of the computational domain in each coordinate direction was $L_X = 15 d_2$, $L_Y = 33.461 d_2$, and $L_Z = 11 d_2$, as shown in Fig. 1. The Reynolds numbers based on the uniform inflow velocity U_o and the diameters d_2 and d_1 were $Re_2 = 40$ and $Re_1 = 22.24$, respectively.

The Navier–Stokes equations in *incompressible* form were solved in 3-D space and time using the *parallel* Finite Volume code MGLET [9]. The code uses a staggered Cartesian grid arrangement and is third order accurate in time (explicit Runge–Kutta scheme) and second order accurate in space (central scheme). The number of grid points in the streamwise (X), spanwise (Y) and cross-stream (Z) directions was $[N_X, N_Y, N_Z] = [224, 200, 170]$. A uniform velocity profile $U_o = 1$ was prescribed at the inlet, and a Neumann boundary condition was used for the pressure. At both the ends of the cylinder and at the top and bottom of the computational domain a *free-slip* boundary condition was used (see Fig. 1). At the outlet, a Neumann boundary condition was used for velocities and the pressure was set to zero.

A *direct forcing* immersed boundary method (IBM) [10] was used to transform the *no-slip* condition at the cylinder surface into internal boundary conditions at the nodes of the Cartesian grid. The solid body (tapered cylinder) to be immersed in the Cartesian mesh was represented by a mesh consisting of triangles. The blocking of the Cartesian cells intersected by these triangles was accomplished as follows:

(i) The intersection points of a triangle surface and the coordinate line passing through the pressure cell centre were identified. The pressure cells containing those intersection points were blocked.
(ii) In a second sweep all the pressure cells within the blocked surface were blocked.
(iii) Finally, all the velocity cells corresponding to blocked pressure cells were blocked.

The internal boundary condition value had to be determined by interpolation. In the present study we used *least-squares* interpolation of third-order accuracy. The detailed derivation, validation and implementation of this technique in the code MGLET were explained in [10].

3 Results and discussion

The numerical solution of the unsteady Navier–Stokes equations converged to a steady state. The present 3-D calculation revealed a modest secondary spanwise velocity V, both in the front stagnation zone and also in the wake of the cylinder (see Fig. 2a–c). It can be observed from Fig. 2a that in the front stagnation zone the secondary flow is going from the wide end of the cylinder towards the narrow end. On the side, i.e. 90° from the front stagnation line, the secondary flow still persists in the same direction although at a lower speed. On the contrary, the secondary motion on the rear side of the cylinder goes in the opposite direction (see Fig. 2b). The magnitude of this spanwise velocity is quite small, typically of the order 1–3% of the inflow U_o. The secondary motion in the spanwise direction is a direct consequence of the three-dimensionality of the tapered cylinder and this kind of secondary flows does not arise in the vicinity of uniform circular cylinders.

The secondary flow is driven by a spanwise pressure gradient. The front stagnation line is slightly inclined with respect to the cylinder axis and this tilt gives rise to a somewhat higher pressure near the wide end of the cylinder as compared to the narrow end. The pressure contours (isobars) in Fig. 3 show that the isobars

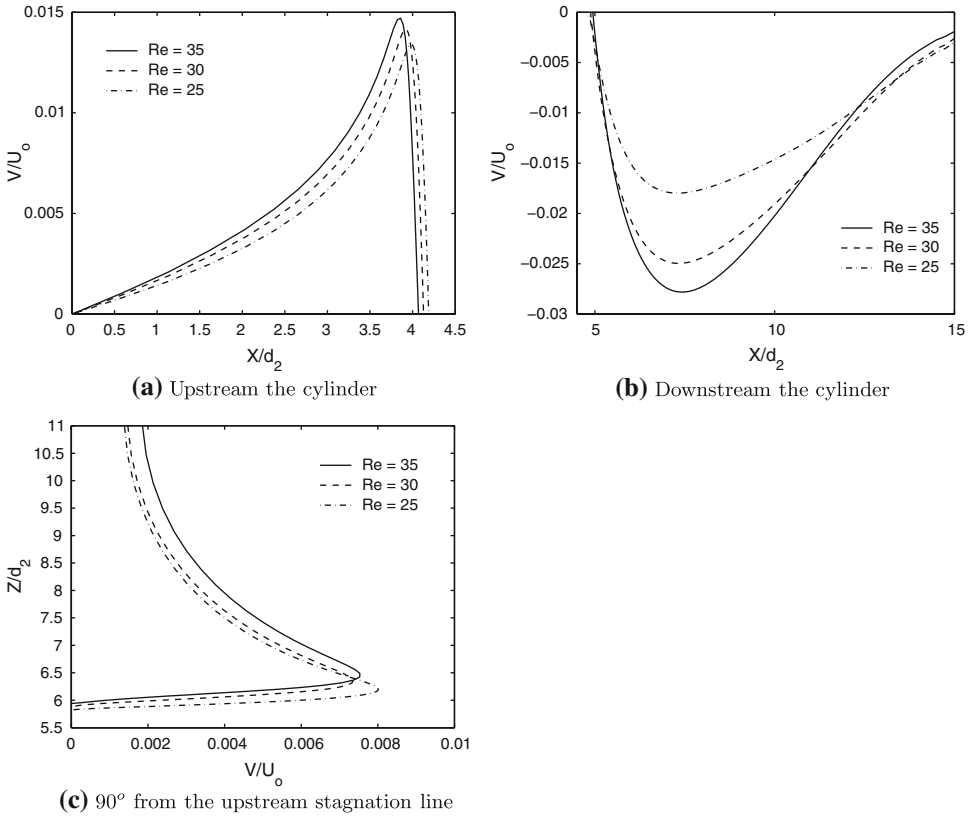

(a) Upstream the cylinder

(b) Downstream the cylinder

(c) 90^o from the upstream stagnation line

Fig. 2 Spanwise velocity V/U_o (secondary flow) at three different spanwise locations identified by the local Reynolds number $Re = U_o d/\nu$. The position of the axis of the cylinder is at $[X/d_2, Z/d_2] = [4.5, 5.5]$

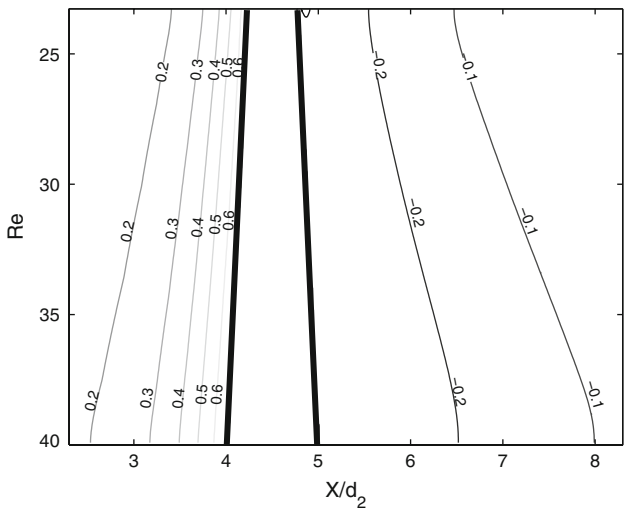

Fig. 3 Pressure $(P/\rho\ U_o^2)$ contours in the $X - Y$ plane through the axis of the cylinder. The cylinder walls are drawn as bold lines

are more inclined towards the cylinder axis than the stagnation line, thereby giving rise to a spanwise pressure gradient which drives the flow towards the narrow end. Similarly, the (negative) isobars in the cylinder wake are also tilted towards the cylinder axis, i.e. the lowest pressure is found in the wake downstream of the widest part of the cylinder. This observation indicates that also the spanwise-oriented flow in the cylinder wake is pressure-driven.

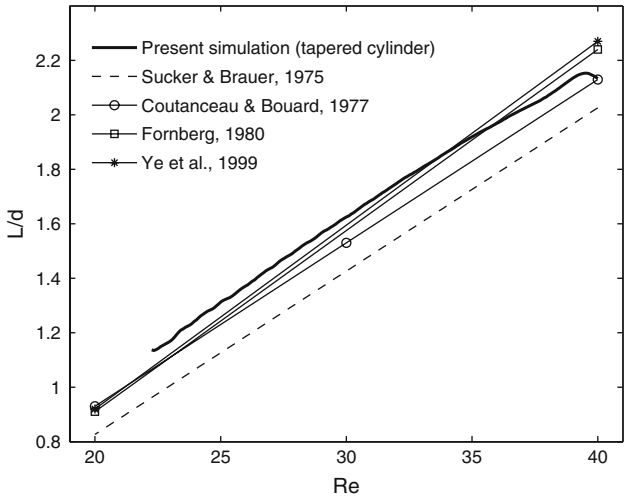

Fig. 4 Non-dimensional length of the steady re-circulation zone (L/d) versus local Reynolds number $Re = U_o\, d/\nu$

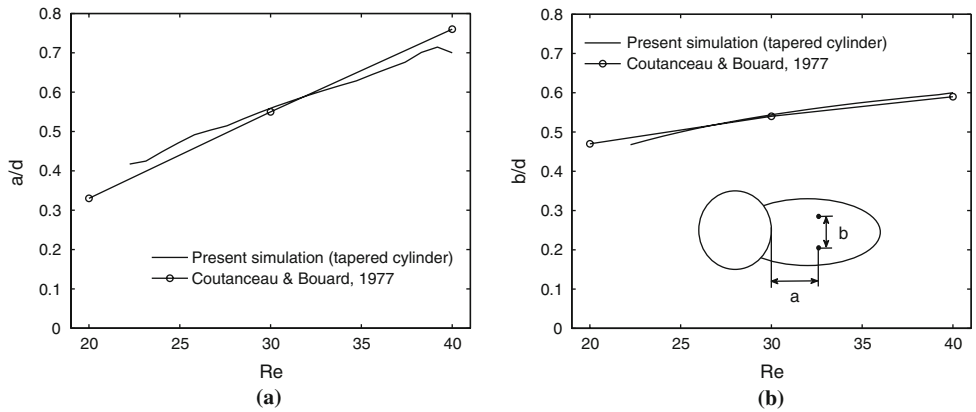

Fig. 5 Position of the re-circulation bubble centre $(a/d, b/d)$ plotted against Re

The constant length L of the closed wake behind a uniform circular cylinder is known to increase monotonically with the Reynolds number in the low-Re regime. Sucker and Brauer [11] deduced the empirical correlation $L/d = 0.12\ Re - 0.748$ on the basis of several experimental and numerical data available at that time. Subsequent data from more refined experiments by Coutanceau and Bouard [12] and computations by Fornberg [13] and Ye et al. [14] and others suggest that the linear correlation due to Sucker and Brauer [11] slightly underestimates the wake length. In the present 3D case, the wake length varies substantially along the cylinder span of the tapered cylinder. In the present context the local wake length L is defined as the streamwise distance from the cylinder surface to the position where the streamwise velocity U changes sign from negative to positive. The wake behind the wide end is roughly four times longer than the wake behind the narrow end of the cylinder. If the local wake length L is scaled with the local diameter d, the spanwise variation of L/d shown in Fig. 4 is surprisingly close to the results for uniform (i.e. 2D) cylinders. The deviation from 2D behaviour is largest near the wide part of the tapered cylinder where the secondary flow is most pronounced (cf. Fig. 2). The coordinate position of the vortex centres (a, b) has been plotted against the local Reynolds number in Fig. 5. Here a is defined as the streamwise distance from the cylinder surface to the vortex centre and b is defined as the cross-stream distance between the two vortex centres. The data from the present numerical study scaled with the local diameter d is in good agreement with the experimental results for uniform (i.e. 2D) cylinders.

4 Conclusion

We have seen that the modest tapering gives rise to a pressure-driven secondary flow along the span of the cylinder. The steady wake exhibits a substantial variation along the span. This variation is associated partly with the variation of the local diameter and partly with the local Reynolds number. The flow field in planes perpendicular to the cylinder axis can thus be considered as quasi-two-dimensional.

Acknowledgments This work has received support from The Research Council of Norway (Programme for Supercomputing) through a grant of computing time. The first author was the recipient of a research fellowship offered by The Research Council of Norway.

References

1. Lewis, C.G., Gharib, M.: An exploration of the wake three dimensionalities caused by a local discontinuity in cylinder diameter. Phys. Fluids A **4**, 104–117 (1992)
2. Vallès, B., Andersson, H.I., Jenssen, C.B.: Direct-mode interactions in the wake behind a stepped cylinder. Phys. Fluids **14**, 1548–1551 (2002)
3. Dunn, W., Tavoularis, S.: Experimental studies of vortices shed from cylinders with a step-change in diameter. J. Fluid Mech. **555**, 409–437 (2006)
4. Gaster, M.: Vortex shedding from slender cones at low Reynolds numbers. J. Fluid Mech. **38**, 565–576 (1969)
5. Piccirillo, P.S., Van Atta, C.W.: An experimental study of vortex shedding behind linearly tapered cylinders at low Reynolds number. J. Fluid Mech. **246**, 163–195 (1993)
6. Vallès, B., Andersson, H.I., Jenssen, C.B.: Oblique vortex shedding behind tapered cylinders. J. Fluids Struct. **16**, 453–463 (2002)
7. Parnaudeau, P., Heitz, D., Lamballais, E., Silvestrini, J.H.: Direct numerical simulations of vortex shedding behind cylinders with spanwise linear nonuniformity. J. Turbulence **8**, 1–13 (2007)
8. Narasimhamurthy, V.D., Andersson, H.I., Pettersen, B.: Direct numerical simulation of vortex shedding behind a linearly tapered circular cylinder. In: Proceedings of IUTAM Symposium on Unsteady Separated Flows and their Control, 2007. Springer, Heidelberg (in press)
9. Manhart, M.: A zonal grid algorithm for DNS of turbulent boundary layers. Comp. Fluids **33**, 435–461 (2004)
10. Peller, N., Le Duc, A., Tremblay, F., Manhart, M.: High-order stable interpolations for immersed boundary methods. Int. J. Numer. Meth. Fluids **52**, 1175–1193 (2006)
11. Sucker, D., Brauer, H.: Fluiddynamik bei quer angeströmten Zylindern. Wärme Stoffübertragung **8**, 149–158 (1975)
12. Coutanceau, M., Bouard, R.: Experimental determination of the main features of the viscous flow in the wake of a circular cylinder in uniform translation. Part 1. Steady flow. J. Fluid Mech. **79**, 231–256 (1977)
13. Fornberg, B.: A numerical study of steady viscous flow past a circular cylinder. J. Fluid Mech. **98**, 819–855 (1980)
14. Ye, T., Mittal, R., Udaykumar, H.S., Shyy, W.: An accurate Cartesian grid method for viscous incompressible flows with complex immersed boundaries. J. Comp. Phys. **156**, 209–240 (1999)